

## PUBLIZIERBARER ENDBERICHT

gilt für Studien aus der Programmlinie Forschung

### A) Projektdaten

<b>Kurztitel:</b>	Deucalion
<b>Langtitel:</b>	Determining and Visualizing Impacts of Greenhouse Climate Rainfall in Alpine Watersheds on Torrential Disasters
<b>Programm inkl. Jahr:</b>	ACRP 2nd call
<b>Dauer:</b>	01.03.2011 – 28.02.2014
<b>KoordinatorIn/ ProjekteinreicherIn:</b>	Dr. Roland Kaitna
<b>Kontaktperson Name:</b>	Dr. Roland Kaitna
<b>Kontaktperson Adresse:</b>	Peter Jordanstr. 82, 1190 Wien
<b>Kontaktperson Telefon:</b>	+43 1 47654 4372
<b>Kontaktperson E-Mail:</b>	roland.kaitna@boku.ac.at
<b>Projekt- und KooperationspartnerIn (inkl. Bundesland):</b>	Dr. Andreas Gobiet, Wegener Center für Klima und Globalen Wandel (WegCenter), Universität Graz, Steiermark Dr. Franz Sinabell, Institut für Wirtschaftsforschung (Wifo), Wien Dr. Markus Stoffel, Labor für Dendrogeomorphologie (Dendrolab), Universität Bern, Schweiz
<b>Schlagwörter:</b>	Wildbachgefahren, Klimawandel, Extremereignisse, Muren, Dendrogeomorphologie, Gefahrenzonenplanung, Risiko
<b>Projektgesamtkosten:</b>	299,889.-€
<b>Fördersumme:</b>	299,889.- €
<b>Klimafonds-Nr:</b>	B060372
<b>Erstellt am:</b>	21.07.2014

## Projektübersicht

### 1 Kurzfassung

Wildbachprozesse wie Hochwasser, Geschiebetransport und Muren repräsentieren ein erhebliches Gefahrenpotential in Alpinen Regionen. Abgesehen von der Grunddisposition eines Einzugsgebietes (z.B. Reliefenergie) und variabler Disposition (z.B. aufgrund saisonaler Veränderungen der Geschiebefüchtigkeit) bestimmt der Regeninput, seien es konvektive oder advektive Niederschläge, das Prozessverhalten. Es ist daher zu erwarten, dass Änderungen des Klimasystems auch Änderungen der Häufigkeit und Magnitude von Wildbachereignissen mit sich führen.

Das Ziel des Projekts „Deucalion“ ist es, mögliche Änderungen von Muren-Ereignissen in Wildbächen aufgrund des Klimawandels zu beurteilen. Zu diesem Zweck wurden die meteorologischen Auslösebedingungen von vergangenen Murenereignissen analysiert und mit Szenarien der Änderungen des Niederschlagsverhaltens verschnitten. In weiterer Folge wurden die Konsequenzen und Unsicherheiten im Zusammenhang mit der Gefahren- und Risikoanalyse in der Ingenieurspraxis untersucht und beurteilt.

Im Projekt DEUCALION wurden drei geomorphologisch und klimatisch unterschiedliche Gebiete untersucht (klimatisch nord-west, süd-west und nord-ost). Das Projekt bestand aus sechs Workpackages (WP), die von vier Partnern (Boku Wien, Universität Graz, Wifo und Universität Bern) abgearbeitet wurden. Die Struktur kann folgendermaßen zusammengefasst werden:

- WP1 – Rekonstruktion und Analyse von Wildbachereignissen
- WP2 – Klimamodellierung
- WP3 – Änderung der meteorologischen Auslösebedingungen
- WP4 – Sozio-ökonomische Entwicklung
- WP5 – Szenarien basierte Modellierung
- WP6 – Projekt Management

Die retrospektive Analyse der Wildbachaktivität in den Untersuchungsgebieten basierte auf der dendro-geomorphologischen Methode und auf Archivdaten. Für die meteorologischen Auslösebedingungen wurden Tages-Daten der nächsten Niederschlagsmessstelle bis maximal sechs Tage vor dem Ereignis untersucht. Für die Klimawandelmodellierung wurden vier regionale Klimasimulationen verwendet, die alle auf einem A1B Emissionsszenario basieren und mittels der empirisch-statistischen „quantile mapping“ Methode Fehler-korrigiert. Dafür wurde zusätzlich eine neue Korrekturmethode entwickelt, um besonders Extremniederschläge korrekt abzubilden.

In einem weiteren Schritt wurden die Auswirkungen von Veränderungen der Magnitude von Muren mittels numerischer Simulationsprogramme getestet und die Unsicherheiten bestimmt. Für einen holistischen Ansatz wurde in einem weiteren Schritt die sozio-ökonomische Entwicklung abgeschätzt und mit in einer Risiko- und Lebenszyklus-Analyse mit den Resultaten der vorangegangenen WPs verschnitten.

Im ersten Schritt wurden insgesamt 1017 Bäume auf 7 Schwemmkegel untersucht. Aufgrund von Wachstumsstörungen in den Jahrringen konnten 44 Muren und 17 Lawinen räumlich und zeitlich rekonstruiert werden. Die Dauer der resultierenden Zeitreihen erstreckte sich zwischen 109 und 142 Jahren. Für die regionale Analyse der auslösenden Niederschläge wurden zusätzlich 1907 Muren-Ereignisse aus den Chroniken verwendet (von 1550 bis 2008). Es zeigte sich, dass 60-90 % der Muren in den Monaten Juni, Juli und August (JJA) zu beobachten waren. Verschnitten mit Zeitreihe des Tagesniederschlags von 48 Wetterstationen konnten minimale, mittlere und maximale Zusammenhänge Intensität und Dauer der auslösenden Niederschläge, basierend auf dem 15%, 50% und 90% Quantil, bestimmt werden ( $I = a \cdot D^b$ ). Für die drei Untersuchungsgebiete variiert der minimale Ereignis-auslösende Tagesniederschlag zwischen 19 und 35 mm, der mittlere zwischen 32 und 59 mm und der maximale zwischen 70 und 100 mm. Höhere Werte wurden in der süd-westlichen Region bestimmt.

Die verbesserte Fehlerkorrektur der regionalen Klimamodelle zeigte eine deutliche Verbesserung der Ergebnisse, besonders bei Extremniederschlägen von kurzer Dauer. Generell zeigt sich ein Trend der saisonalen Verschiebung extremer Niederschläge in das Frühjahr und den Herbst.

Verschnitten mit den Grenzwerten der Ereignisauslösung konnte für das „beste“ Klimaszenario und alle Untersuchungsgebiete praktisch keine Veränderungen im Mai und Juni und einen Rückgang der Wahrscheinlichkeiten im Juli und August festgestellt werden. Beim „schlechtesten“ Szenario wurde ein Anstieg der Wahrscheinlichkeit in manchen Zeiträumen in allen Gebieten errechnet. Die Szenario-basierte Modellierung von Muren zeigte einen relativ geringen Einfluss der Ereignisgröße im Vergleich zur Unsicherheit der Modellparameter für alle drei Untersuchungsgebiete. Durch die anschließende Szenario-basierte Risiko- und Lebenszyklusanalyse wurde die große Bedeutung von Schutzmaßnahmen und deren Erhaltung gezeigt.

## 2 Executive Summary

Torrential processes like flash floods, debris flows, and debris floods represent a serious hazard in Alpine environments. Apart from the basic disposition of a watershed (e.g. relief energy, sediment availability) and variable disposition (e.g. seasonal changes), the trigger of these events are mostly intense convective storms or advective rainfalls. Therefore changes of climatic conditions are likely to have direct and potentially drastic impacts on the frequency and ensuing magnitude of torrential disasters.

The aim of the "DEUCALION" project is to assess changes of potential future disasters for different alpine watersheds based on retrospective analyses and predictions of changes of triggering conditions. The main contribution of the project is a better assessment of past, contemporary and potential future torrential hazards and subsequent assessment of associated risks for human assets on vulnerable fans and cones.

Within the DEUCALION project we analyzed three characteristic study regions, representing different geomorphic settings and characteristic climatic influences (North-west, south-west, and north-east). The project team comprises four partners (IAN-Boku Vienna, WegCenter Univ. Graz, Wifo, and Dendrolab Univ. Bern) that work in six work packages (WP). The structure can be summarized as:

- WP1 – Reconstruction and analysis of torrential events
- WP2 – Evolution of rainfall in the watersheds
- WP3 – Assessment of changes of torrential processes
- WP4 – Socio-economic development
- WP5 – Modeling of torrential events
- WP6 – Project management

The retrospective analysis of torrential activity was performed by extensive tree-ring analysis and geomorphic mapping, as well as through the gathering of archival data on event frequency and magnitude of past events. The subsequent assessment of triggering factors of past torrential events was based on tree-ring data and the Austrian Natural Disaster Database as well as daily time series from nearest meteorological stations. To assess possible changes of trigger conditions, 4 regional climate simulations (based on an A1B emission scenario) were error corrected using an empirical-statistical quantile mapping (QM) approach. A new combined parametric and nonparametric correction method for precipitation with an extension for new extremes was developed, implemented and compared with the original non-parametric QM method. Subsequently scenario-based modeling of debris flow activity at each case-study site was carried out to assess possible impacts of climate change compared to model uncertainty. To reflect the holistic approach current socio-economic and demographic states at our study sites were analyzed and scenarios for future developments determined. Finally a combined risk- and life cycle assessment for a selected study site was carried out.

In total we investigated the tree ring sequences of 1017 trees on 7 debris flow fans in our three study regions. Analyzing growth disturbances allowed a spatial reconstruction of 44 past debris flow events and 17 snow avalanche events. The reconstructed event series covered at least one century (MIN: 109 yrs, MAX 142 yrs).

For a regional assessment of meteorological trigger conditions of the past, a total of 1907 events (dating from 1559 to 2008) were analyzed. We found that 60 – 90 % of the debris flow events occurred on the month June, July and August (JJA). Connected with daily precipitation time series

of 48 meteorological stations we identified minimum, medium and maximum threshold relations (reflecting the 15th, 50th and the 90th percentile of the data) between rainfall intensity and duration ( $I = a \cdot D^b$ ). For our three study regions, the minimum threshold of daily precipitation varies between 19 and 35 mm, the medium between 32 and 59 mm and the maximum between 70 and 100 mm. There was evidence that thresholds are highest in the south-west region.

For climate change modeling an improved bias correction method for extreme precipitation was developed, implemented and evaluated. According to the cross validation frame work, it was found that the new method is capable to improve the representation of new extreme precipitation events in several cases.

Connecting climate change modeling with the earlier identified thresholds we found that for the "best" climate change scenario there is almost no change of debris flow probability in all study regions from May to June, and a decrease in July and August. For the "worst" climate change scenario we found an increased probability for some seasons in all regions, especially in summer and in the north-east.

Scenario-based hazard modeling, based on variation of event volumes, showed only minor influence on the hazard zones for our three test sites. Scenario-based risk and life cycle modeling reveals the importance of mitigation measures, which have a strong effect on the predicted costs.

### 3 Hintergrund und Zielsetzung

Debris flows represent a serious hazard for human settlements and infrastructure in alpine regions. Apart from the basic disposition of a watershed (e.g. relief energy, sediment availability) and variable disposition (e.g. seasonal changes), the trigger of these events are mostly intense convective storms or advective rainfalls. Therefore changes of climatic conditions are likely to have direct and potentially drastic impacts on the frequency and ensuing magnitude of torrential disasters. Up now there is no quantitative study of potential changes of magnitude and frequency of debris flow activity in the Austrian Alps. Therefore, the aim of the "DEUCALION" project was to assess changes of potential future disasters for different alpine regions and assess the consequences for selected watersheds. The main contribution of the project is a first time combined assessment of past, contemporary and potential future threshold conditions and subsequent assessment of changes of associated risks for human assets on vulnerable fans and cones

### 4 Projektinhalt und Ergebnis(se)

#### WP 1: Creation of time series on torrential processes: frequency and magnitude, triggers and impacts

Field sites were selected in three greater Alpine regions: northwest (Pitztal), northeast (Gesäuse) and southwest (Toblachersee) (Figure 1). The study site Gesäuse is of special interest, since it comprises five separate gullies, which were sampled and analyzed separately to first time evaluate the reaction of very small neighboring watersheds (within a total distance of 2 km) to similar rainfall inputs over long time-scales. To use synergies, the Wartschenbach torrent (Lienz, Eastern Tyrol), which is located in the south-west region was included into the analysis. At the Wartschenbach torrent out of the eleven known events, nine debris flows were documented during the period 1995 and 2000, including information on event volume and meteorological trigger conditions. An overview of the main geomorphic characteristics of the four watersheds is given in Table 1.

To reconstruct the history of past events on the cone of the Reiselehnrinne, Gesäuse and Toblachersee, a total of 1017 trees obviously influenced by past torrential activity (scars, exposed root systems, tilted stems or buried stem base) were sampled. Afterwards the increment cores were analyzed in the laboratory following the standard dendrogeomorphic procedures described by Stoffel and Bollschweiler (2008, 2009). Finally growth disturbances, such as tangential rows of traumatic resin ducts, callus tissue, injuries, sudden growth suppressions or releases and compression wood allowed the reconstruction of past events with annual resolution (see Table 2).

In the Pitztal we could reconstruct 8 debris flow events and 17 snow avalanche events, at Toblachersee 17 debris flow events and at the Gesäuse site 19 debris flows within 5 gullies (Kogelnig-Mayer et al. 2011, Schraml et al. 2012, Schraml et al. in review). The reconstructed event series cover at least one century (MIN: 109 yrs, MAX 142 yrs).

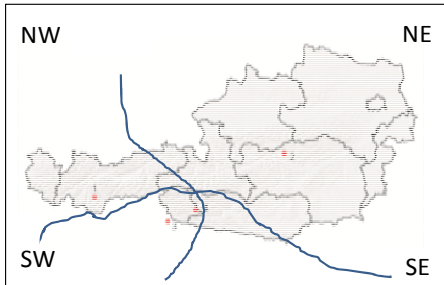


Figure 1: Location of the selected cones (1: Reiselehnrinne; 2: Gesäuse; 3: Toblacher See; 4: Wartschenbach)

Torrent	Catchment size	Geology	Mean slope angle	Elevation (ASL) of the cone
Reiselehnrinne	0.7 km <sup>2</sup>	Gneiss & Schists	23 °	1600 m
Gesaeuse - 1	0.6 km <sup>2</sup>	Dolomite	7 °	650 m
Gesaeuse - 2	0.7 km <sup>2</sup>	Dolomite	9 °	650 m
Gesaeuse - 3	0.3 km <sup>2</sup>	Dolomite	8 °	650 m
Gesaeuse - 4	0.4 km <sup>2</sup>	Dolomite	12 °	650 m
Gesaeuse - 5	0.4 km <sup>2</sup>	Dolomite	8 °	650 m
Toblacher See	0.6 km <sup>2</sup>	Dolomite	12 °	1250 m
Wartschenbach	2.7 km <sup>2</sup>	Crystalline	12 °	1460 m

Table 1: Catchment size, geology and slope angle of the selected study sites

Table 2: Number and age of sampled trees for each cone and number of events per cone.

Torrent	No. of trees sampled	Average tree age	No of growth disturbances	First datable event	No. of years with torrential activity (reconstruction + archives)
Reiselehnrinne	372	88 years	735	1868	8 (+ 17 snow avalanches)
Gesaeuse	384	74 years	3164	1903	19
Toblachersee	261	123 years	730	1888	17
Wartschenbach	-	-	-	1870	11

Using data from meteorological stations closest to the investigated torrents (five stations were analyzed for Toblach covering the period 1922-2011, three for Gesäuse (concentrating on the period 1971-2009), and one for Pitztal (1918-2009)) we conducted an analysis based on logistic regression to infer local rainfall thresholds. We found limited significance and a high sensitivity to extremes.

A regional analysis of rainfall threshold conditions was based on additional data from a unique database of past debris flow events (Austrian Natural Disaster Database). In total 1907 events (dating from 1559 to 2008) in all three regions (clustered in 5 sub-regions: Hochberg, Gesäuse, Landeck, Lienz and Kitzbuhel) were analyzed. Figure 2 shows the spatial distribution of all events in these sub-regions and seasonal histograms.

We see that the majority of events occurred between 1960 and 2008, which is due to a low documentation activity in early years. We found that 60 – 90 % of the debris flow events occurred on the month June, July and August (JJA), with a similar behavior in each region.

Using daily precipitation time series of 48 meteorological stations (covering the period 1895 to 2008) we analyzed the daily intensity and duration of precipitation events leading to debris flow triggering. Each catchment was associated to the closest meteorological station of this network. As, on days with temperatures below 5°C, the amount of water provided by precipitation is temporarily stored as snow in the upper part of the catchments, the events that occurred during snowy days were removed from the analysis. For comparative reasons we calculated a precipitation day normal (PDN) for each region, using  $PDN = MAP / APD$ , where MAP is mean annual precipitation, and APD is average precipitation days per year.

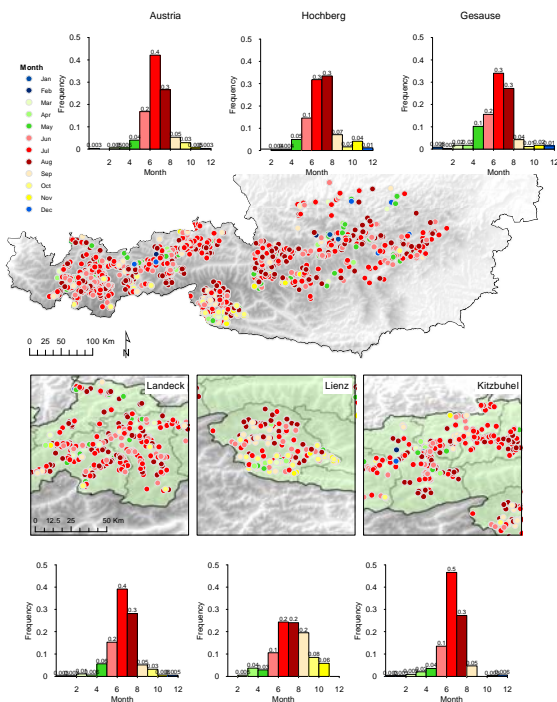


Figure 2: Overview of all dated debris flow events in the investigated sub-regions. The histograms above and below the map represent the distributions of events in the period between 1559 and 2008.

To define a valid intensity-duration (ID) threshold, it is necessary to determine the critical intensities related to durations of the rainfall events, which triggered debris flows. The choice of the duration is often done by a subjective definition of the triggering events, e.g., from the approximate point in time where heavy rainfall started (Guzzetti et al., 2007). In order to define event durations more objectively, we extracted the relevant time-dependent data directly from the meteorological dataset. Thereby we obtained the critical duration by using the maximum average intensity [ $\text{mm day}^{-1}$ ] prior to each debris flow event, also known as the maximum antecedent water supply  $ID = \max(WSC / D) \sim D$ , where ID is the intensity-duration relationship used for threshold definition, WSC is the cumulative water supply in the time period prior to the debris flow and D is the corresponding duration in days. Intensity-duration relationships were calculated for each day in 6 days in advance of each debris flow event and the maximum value was chosen for threshold definition.

The intensity-duration (ID) relationships for the 1907 debris flow events served as input for the definition of minimum, medium and maximum thresholds. All three threshold levels are calculated for the absolute and normalized intensities over a range of 1 to 6 days and can only be applied over this period of time. The absolute threshold plot shows the absolute intensity [ $\text{mm day}^{-1}$ ] over the corresponding duration (Figure 3 left), while the normalized plot shows the absolute intensity [ $\text{mm day}^{-1}$ ] divided by the local precipitation day normal (PDN) and plotted against the duration (Figure 3 right). As noted before, normalization was carried out to account for differences in local climate. The minimum threshold was obtained by calculating the 5th and the 15th intensity percentiles for 1 to 6 days duration. The method used for the definition of the medium and maximum thresholds was similar. The medium threshold aims to capture 50 % of the obtained ID relationships. The maximum threshold aims to capture 10 % of the ID relationships. Within DEUCALION, the minimum threshold is interpreted as the "safety threshold", the lowest intensity-duration relation that is able to trigger debris flows. The medium threshold is interpreted as the intensity-duration relation that is likely to trigger debris flows, whereas the maximum threshold indicates the intensity above which debris flows will always occur (e.g. Guzzetti et al., 2007). The absolute ID thresholds obtained for the whole Tyrol region are represented, for instance, in Figure 3.

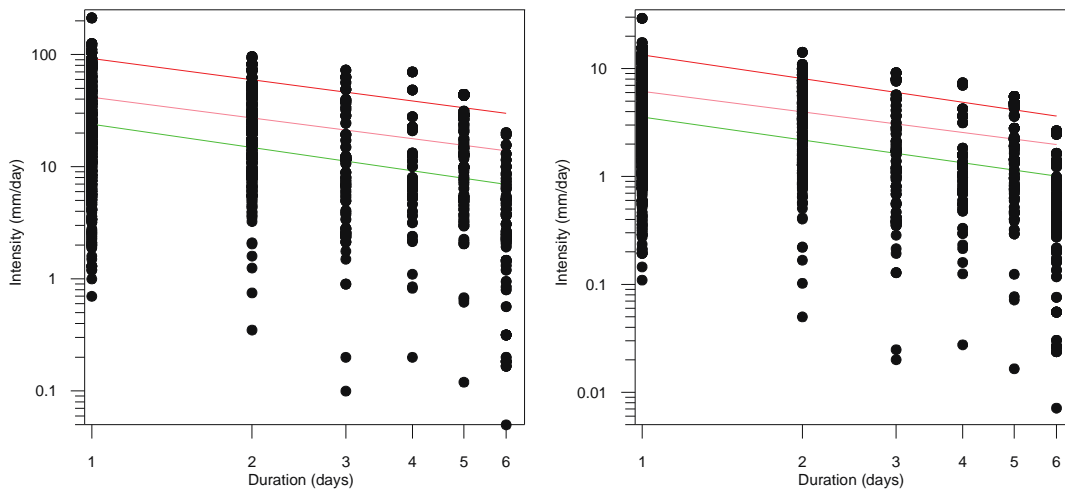


Figure 3: Absolute (left) and relative (right) ID threshold curves for debris flow initiation obtained from the intensity 1-day moving average of the 5th and 15th percentiles (minimum threshold), the 45th and 55th percentiles (medium threshold) and the 85th and 95th percentiles (maximum threshold).

Absolute precipitation intensities were calculated from ID curves over durations of 1, 3 and 5 days, for all regions (Figure 4). Minimum absolute 1-day precipitation thresholds vary between 19 (Hochberg) and 35 mm (Lienz) while minimum 5-day precipitation threshold range between 3.3 and 16 mm though reproducing the negative exponent. Generally, higher thresholds are computed in the central and southern parts of Tyrol (Kitzbuhel, Lienz). We also calculated relative ID thresholds, which were normalized by the precipitation day normal. Generally our results are comparable to those obtained with less data from Carinthia and Eastern Tyrol (Moser and Hohensinn, 1983) and in several alpine regions (e.g. NE Alps in Italy - Paronuzzi et al., 1998). It has to be considered that all given thresholds were derived on the basis of daily precipitation values. Local thresholds values are expected to be significantly higher.

#### WP 2: Evolution of mean / extreme rainfalls in torrential watersheds based on statistically downscaled RCM ensemble data

The main objective of WP2 was to derive localized future scenarios of climate parameters triggering torrential disasters and to quantify uncertainties. As input for the analysis of future torrential activity within the DEUCALION project reliable localized scenarios of heavy precipitation events are required. In order to improve the reliability of the scenarios, regional climate simulations were error corrected using an empirical-statistical quantile mapping approach (QM, Themeßl et al. 2011, 2012; Wilcke et al., 2013, 2014). This approach proved to have a high correction potential for extreme precipitation, but at the same time has room for further improvements, in particular with regard to "new extremes", i.e. extreme events that were not observed in the past, but could occur in future. Along with global warming until the end of the 21st century, new extremes outside the ranges observed in the past are likely to occur (IPCC, 2001, 2007; van der Linden and Mitchell, 2009). This motivated to extend the QM method to produce more reliable scenarios for new record breaking precipitation extremes. The main objective of this work is to develop such a method and to assess its performance.

Fitting theoretical distributions to the entire empirical distribution of data (e.g., Piani et al., 2009; Dobler and Ahrens, 2008) would be one way to extrapolate the correction beyond the observed range, but this would lead to loss of information compared to using the empirical distribution, as well as to a limitation of flexibility of QM, which can be applied to any meteorological variable, as long as empirical distributions are used. By considering these arguments, we fit a theoretical distribution only for high extremes and use the empirical distribution for the major part of the data.

The main advantage of this approach is that it can easily be adapted to any meteorological variable. The new combined parametric and nonparametric bias correction method ( $QM\beta$ ) was developed for precipitation, implemented and compared with a non-parametric  $QM$  method ( $QM\alpha$ ). A detailed methodological description about new method is given in the methods section. We evaluated the results to examine the quality of the new method using split sample and cross validation approaches.

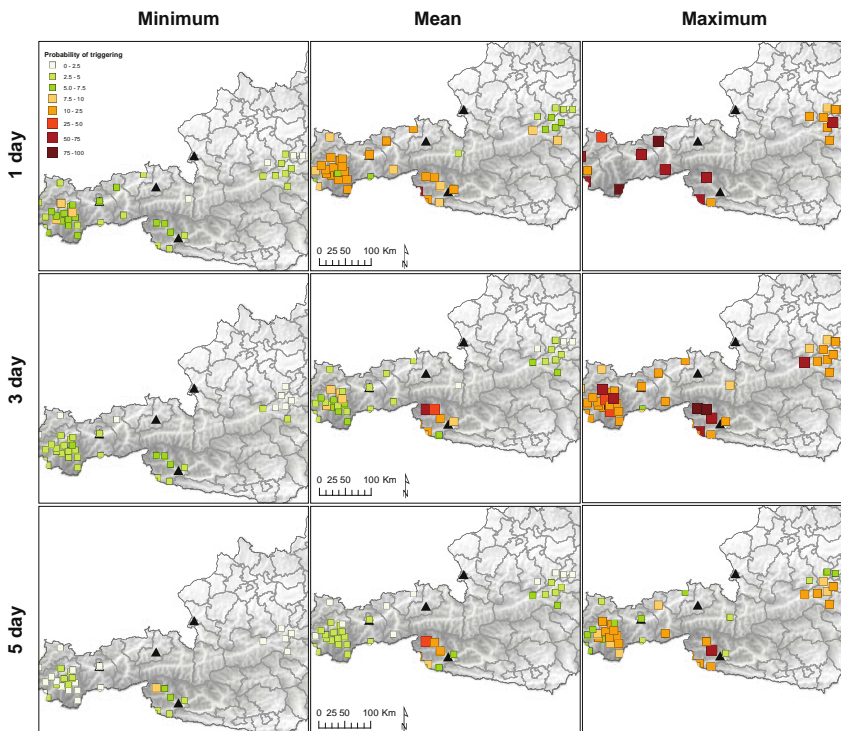


Figure 4: Probability of debris flows triggering in case of minimum (left column), mean (center) and maximum (right column) exceedance during 1 (upper panel), 3 (central panel) or 5 days (lower panel).

*Correction function:*

As a first step to analyze the behavior of the new bias correction approach explained in the methods section, we compared the correction functions of the three methods  $QM\alpha$ ,  $QM\beta_0$ , and  $QM\beta_1$ . Daily correction functions are constructed using model and observation data for all stations in the study area, using a sliding window of 30 days and the period from 1971 to 2007. For illustration purposes, we show the correction functions of day 15 of each month in Figure 5. In order to display also the correction function for new extremes, we added 10 mm precipitation to the model maximum precipitation value. Figure 5 demonstrates the unstable behavior of correction function at higher quantiles with  $QM\alpha$  during the months of April, May, June, October and November, whereas correction function for  $QM\beta_0$  and  $QM\beta_1$  are smoother. In most cases  $QM\beta_0$  and  $QM\beta_1$  yield identical results, but very high correction values are found for  $QM\beta_0$  in the January, where  $QM\beta_1$  helps to maintain reasonably low correction values.

ISB - C4IRCA3-CTL - W 30 - Day15

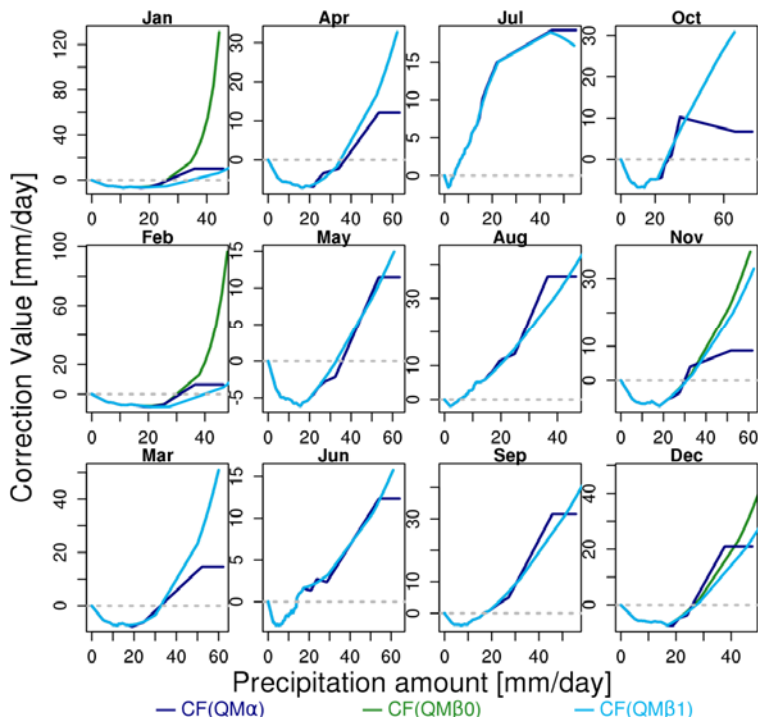


Figure 5: Daily correction functions of the three quantile mapping methods (QM $\alpha$ , QM $\beta$ 0 and QM $\beta$ 1) for station Iselsberg-Penzelberg (ISB), Austria.

*Split sample test*

In a split sample test independent validation and calibration periods are used. In our case, the calibration period is 1971-1990, whereas the data are validated in the independent period 1991-2007. This split-sample approach mimics the application to future climate scenarios, where observations of the past are used to calibrate methods that are applied to simulations of the future. We generated the results of the split sample evaluation as q-q and frequency bias plots. Frequency based evaluation has been carried out for various precipitation thresholds and all stations. As example, the results for precipitation events of more than 10, 30, 50, and 60 mm/day at station Admont (ADM), Austria are shown in Figure 6. For thresholds larger than 30 mm/day, the performance of the bias correction method QM $\alpha$  (navy blue) starts to degrade. The median and spread is reduced above 30 mm/day precipitation events with both QM $\beta$ 0, QM $\beta$ 1 bias corrected methods. QM $\beta$ 1 bias corrected method performs slightly better than QM $\beta$ 0 in reducing frequency biases.

WP 3: Changes in frequency and magnitude of torrential events in a future greenhouse climate

Changes in rainfall intensity and duration, in combination with higher temperatures, are thought to lead to increased frequency of debris flows, provided that sediment is not limited and that the occurrence of events is driven above all by water input above a certain hydroclimatic threshold (e.g., Guzzetti et al., 2007). Based on the historical database used for past analysis and on point-based downscaled climate scenarios for meteorological stations located next to the catchments, we study the evolution of debris flows events above specific thresholds (from 10 to 100 mm) and durations (1, 2 or 3 days) for the period 2012-2050.

For the future, projections from 24 different scenarios (22 Regional Climate Models (RCM) from ENSEMBLES and 2 RCM from RECLIP) were used for 10 meteorological stations, for 2 months periods to fully assess the range of climate model uncertainty. Results indicate changes (in percent) in the number of days with >10 to 100 mm daily liquid precipitation. In order to make predictions about the number of events in a future climate, events in 30, 50 and 100 km buffers around each meteorological station have been extracted from the historical database. The 100 km

buffer is the only one that has been retained. Indeed, it permitted to associate a sufficient number of torrents to each meteorological station and to derive statistically significant relationships between precipitation threshold exceedance and debris flow triggering in past and future climates. In order to homogenize the dataset, only events during the period 1950-2000 were retained from the database. In each 100km buffer, the average rainfall intensity [mm day<sup>-1</sup>] from 1 to 3 days prior to each debris flow event was computed.

For each threshold (from 10 to 100 mm) and for each duration (from 1 to 3 days), the number of events over threshold was computed. Finally, the number of events in a future climate was predicted according to the best and worst scenarios by multiplying the number of events over thresholds by the number of events predicted by these scenarios. Figure 7 summarizes, as an example, the analysis for months May-June at Iselberg Penzelberg meteorological station but similar matrixes (not presented here) were computed for each meteorological station and for 2 months periods from May-June to Sept-Oct.

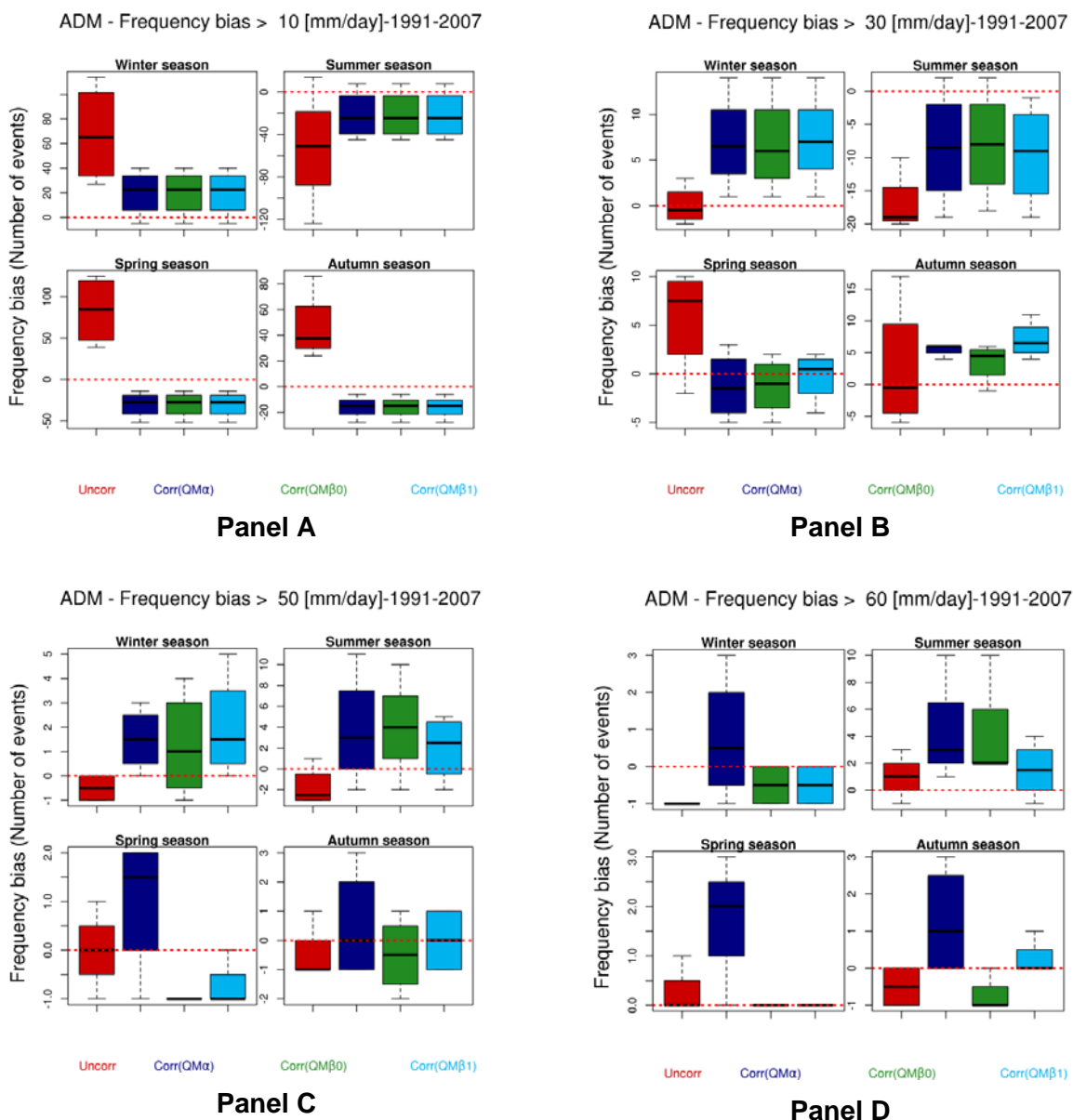


Figure: 6: Biases in the frequency of days with more than 10, 30, 50, and 60 mm/day precipitation of 4 RCM simulations at station Admont (ADM), Austria for three QM methods. Box and whiskers indicate the variability of frequency bias. Boxes indicate the first (q25) and the third (q75) quartile,

the whiskers extend to q5 and q95, and the black horizontal line indicates the median. The dashed redline indicates zero biases in frequency of days.

According to Figure 7, in the 100 km buffer around Iselberg-Penzelberg station, the number of events triggered by 1 day precipitation > 40 mm was 0.4 events / decade between 1950 and 2000. According to the best scenario from RCM (WEGC-CCLM\_ECHAM5-A1Br2\_DS\_10km\_1955-2050), the number of events will decrease to 0.23 events/decade in 2050. Conversely, within the worst predictions (obtained with CNRM-RM5.1\_SCN\_ARPEGE\_DM\_25km\_1951-2050) the number of events will increase to 1.2 events/decade in 2050. Similarly, the matrix reveals a sharp increase in the number of events triggered by 2 and 3-day precipitation above 10 mm (from 1.6 to 2.17 and from 1.6 to 2.2 events/decade respectively). At the station scale, the sum of the matrixes for each of the three rows corresponds to the number of events triggered by 1, 2 and 3-day precipitation regardless the threshold. In a 100 km buffer around Iselberg-Penzelberg, the number of events triggered by 1-day precipitation, in May-June, will though increase from 3.4 events/decade for the reference period 1950-2000 to 4.9 events/decade according to the worst predictions. Conversely, this frequency will only decrease to 3.2 events/decade on the basis of the best scenario. In a manner similar to that developed at Iselberg-Penzelberg, matrixes that synthetized the changes in the number of debris flow events in 100 km buffers around each meteorological station retained for analysis have been produced on the basis of the best and the worst scenarios available from RCM.

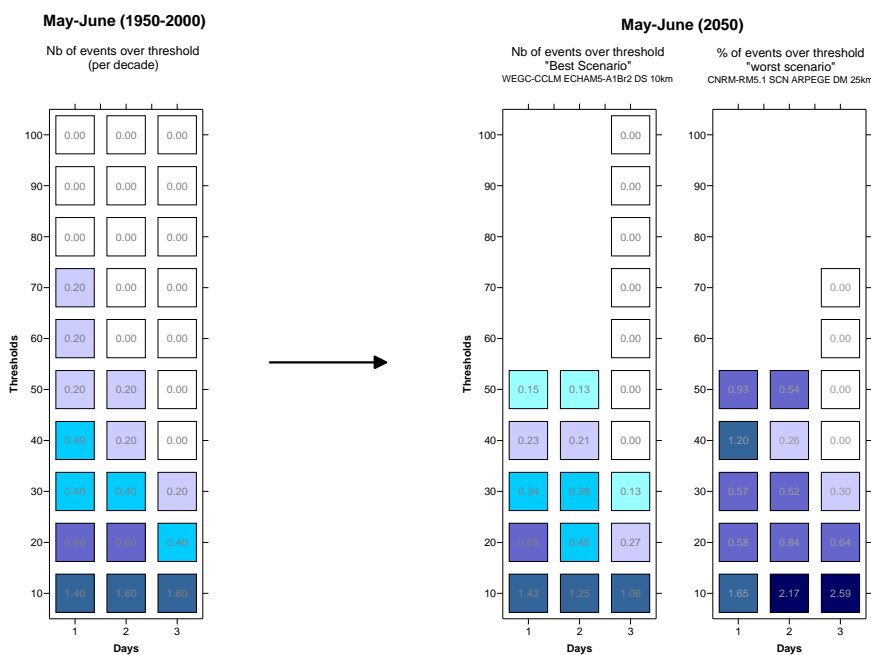


Figure 7: Evolution (2050) of the number of events at Iselberg-Penzelberg meteorological station according to RCM "best" and "worst" simulations

Results show that in the past the number of events in May-June ranged between 2 (region Liezen) and 7 events/decade (region Pitztal). In the future, according to the best scenario, no significant change will be observed. Conversely, referring to the worst scenario, the number of expected events will range between 2.1 events/decade (region Liezen) and 7 events/decade for the region representative for Kirchenlandl.

Uncertainties still exist about the evolution of debris flows in June-July (central panel). Indeed, in the past, the number of events in the past ranged between 7.6 (Liezen) and 12.8 events/decade (Gstatterboden). In the future, according to the best RCM scenario, the number of events will significantly decrease (from 5.4 events/decade in Liezen to 8.1 events/decade in Gstatterboden/Gesäuse region). Conversely according to the worst scenario, major changes will be

observed, especially in Gesäuse area (15.9 events/decade in Admont, +76%; 21.2 events/decade in Gstatterboden, +68%; 17.1 events/decade in Kirchenlandl, +62%).

The event magnitude of a debris flow depends on a wide range of factors, including relief energy, sediment availability in the starting zone and erosion potential in the transit zone, and water input (trigger conditions). We assessed sediment availability for our study sites by field investigations and aerial photography using an unmanned aerial vehicle (UAV). We found indication that the field site "Wartschenbach" is characterized by high sediment availability due to potentially intensive erosion in the transit zone. The site "Reislehnrinne" in Pitztal shows abundant material for entrainment, which therefore might be only limited by water availability. On the other side, mass wasting processes at the "Gesäuse" site seem to be fed by recent weathering processes, i.e. we consider this as a transport limited system. To roughly quantify a potential change of future debris flow event magnitude we assume unlimited sediment availability in our study sites and expect that a change of debris flow event volume directly scales with a change of design peak discharge (i.e. a higher discharge leads to more erosion). We carried out a hydrologic modeling with an ensemble of five climate change projections (Eckhart et al. 2013) and subsequently define scenarios for debris flow impact assessment with + 25 %, and additionally a worst case scenario of + 100 %.

WP 4: Socio-economic developments at study sites and related changes in vulnerability

In the socio-economic analyses the concept of vulnerability was explored for the test sites (Sinabell 2014). The research question was: What kind of information and decision support is needed in order to allocate public funds in a cost-effective manner and which socio-economic developments have to be considered. Two aspects were considered in more depth: population dynamics and attrition of protective constructions. The results of WP 4 were used in the risk and life-cycle assessment in WP 5.

Evidence on the number of potentially vulnerable objects (houses, premises) was collected and maps were developed that show the vulnerability towards floods and debris flows. The milestones achieved in this analysis were overviews of vulnerability of objects that combine the number of objects at risk with the level of protection offered by torrent control constructions (see Figure 8 as an example). Such an overview on the combination of vulnerability and levels of protection has not been made prior to this analysis.

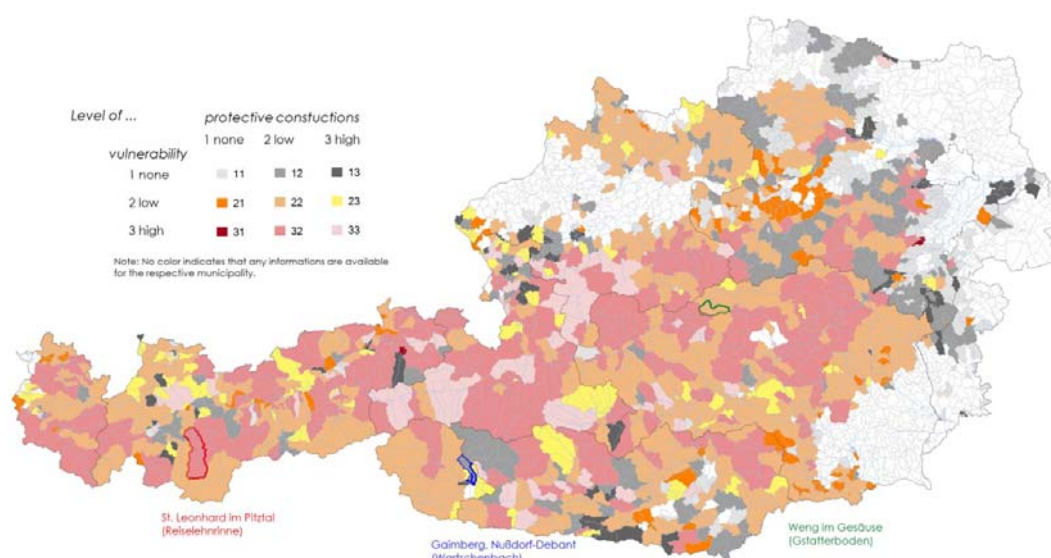


Figure 8: Clusters of municipalities according to the level of protective constructions and the level of vulnerability (source: own construction based on, Sinabell, et al., 2009 and Fuchs and Zischg, 2013, p.75): vulnerability high - more than 100 objects per municipality are vulnerable, low 1-99 objects are vulnerable; protective construction: high - index level in 2008 from 0.5 to 1 (fully installed protection concept), low - index level minor 0.5, none - undeveloped catchment area. Disclaimer: In some municipalities hazard zones are not available electronically. In such cases

vulnerability is indicated to be "1 none". In these few cases this does not mean that no houses/persons are at risk but that no information is available.

Figure 8 shows the municipalities of the test sites and clusters of municipalities according to the level of protection provided by investments in torrent control constructions (based on Sinabell et al. 2009) and according to the level of objects at risk concerning debris flows (as defined by Fuchs and Zischg, 2013). This figure depicts a link between torrent control constructions and the number of vulnerable objects (premises, houses, buildings). The map is not yet an indication of regions where further or new investments could be indicated based on cost-effectiveness criteria. Nevertheless it shows a route of rational resource allocation at the macro-level that should be considered in decision making when public funds are allocated in order to provide hazard control investments. The colors in Figure 8 have to be interpreted with care because it links two types of information that are not on the same scale. Vulnerability is a concept that is related to costs and benefits. The information on protective constructions in torrent catchment areas does not say anything about costs; it is mere technical information. It may be very cheap to construct a very effective control in one region on the one hand. On the other hand it may be extremely expensive to provide at least a little protection in another region. This may likely be the case in regions that are shaded in grey. This hypothesis can be tested once more information on the spatial distribution of investments in monetary terms is available.

Figure 12 displays that there are practically no municipalities where vulnerability is high and protective constructions are non-existing (see disclaimer in the footnotes of the figure). In most cases vulnerability is low and the level of protection is either low or high. This would be the expected outcome of a decision making process that allocates investments over a broad spatial dimension. In order to use this information in a forward looking manner projections on the future developments have to be considered, not only the current situation.

The analysis shows that vulnerability is not a static but a dynamic concept. One dynamic aspect is presented in Table 3 which shows projections on population growth and decline for counties (Länder) and selected districts in Austria. The study regions are different – not only with respect to the exposure to hazards – but also with respect to expected changes. In the Gesäuse region population declined by 3.5 % between 2001 and 2011. This trend will go on until 2030 for Benchmark scenario (constant fertility, life expectancy and immigration) and the main scenario (mean fertility, life expectancy and immigration). Only for the growth scenario (high fertility, life expectancy and immigration) no major changes in population dynamics are expected. In the Pitztal region we see an opposing trend and population growth will go on for all scenarios. The Lienz region shows a less pronounced trend. Such differences should be accounted for when decisions on protective investments will be made.

In order to evaluate how vulnerable people are, efforts have to be undertaken in order to establish reliable decision support systems. At the moment the level of information is much better than it was a decade ago but not yet good enough. One finding is that it is currently well understood how many objects and persons are vulnerable to various sources of risk (e.g. floods and debris flows). An aspect that needs further exploration is the attrition of protective constructions. It is a fact that a given level of protection (due to protective investments) is not there for all times. Attrition of protection constructions and damages due to events with high impact, bring about a gradual and ongoing loss of protection. This process can be retarded by maintenance and repair, which is also costly but may be worthwhile depending on the level of vulnerability.

The fact that protective constructions lose their protective capacity over time due to attrition and due to damaging events and the fact that population changes and that the economy develops have to be considered in addition to the consequences of climate change, as demonstrated in the risk and life-cycle assessment in WP 5. Potential effects of climatic change on the frequency and impact of hazardous events need to be put into a coherent framework of dynamic analysis. An exploration of socio-economic developments at the study site is one element of such an analysis.

Based on forecasts of population dynamics that are available at the level of districts it is possible to make educated assumptions about the future numbers of inhabitants in the municipalities where study sites are located. Estimates on the future number of houses can be derived from the

expected number of inhabitants with some degree of uncertainty. By looking at the number of inhabitants in the past and comparing it with future developments in the district gives indications on possible future scenarios of socio-economic developments.

Decisions on investments in protective constructions are currently not considering such dynamic processes in a forward looking manner. A better use of public funds therefore calls for better decision support system by those who are in charge of allocating funds to projects that promise the highest social benefit.

#### WP 5: Retrospective and scenario-defined modeling of selected torrential disasters and assessment of risks

Spatio-temporal data on torrential disasters, as obtained from growth-ring records of disturbed trees, geomorphic field work and from archival event documentation (WP1), were used to replicate recent events at our study sites using numerical simulation tools. These retrospective modeling can be regarded as "calibration runs", which was the basis for quantification of the effect of potential changes of endangered area due to changes of event magnitude. Additionally we compared the results from scenarios defined in WP3 with the sensitivity of model parameterization. In the Deucalion study we employed the classic engineering simulation tool Flo2D for the Wartschenbach site, and compared the newly released simulation program RAMMS-DF with the not yet commercially available code DAN3D at the study sites Reislehrinne and Gesäuse. To enhance the impact of the study, we collaborated directly with the RAMMS-DF and DAN3D developers. The activities included a three-week research visit at the WSL research institute of the ETH Zuerich to define the specific parameters and set up simulations as realistic as possible. For all simulations tools in common is the solution of depth averaged flow equations and a one-phase constitute equation defining flow dynamics (Bingham-type approach for Flo2D and a Voellmy-type model for RAMMS-DF and DAN3D (selected)). Details, including specifics on the numerical solution algorithms can be found in O'Brien et al. (1993), Hungr & McDougal (2009), Christen et al. (2010).

We find that all models reasonably well reproduce the observed deposition pattern once calibrated. Figure 9 illustrates the sensitivity of model parameters for RAMMS-DF and DAN3D (Voellmy parameters  $\mu$  and  $\xi$ ) compared to the sensitivity of event magnitude. As we see that in all simulated scenarios the flow reaches the county highway (critical infrastructure), but never reaches buildings. We also find that a variation of the friction parameter  $\mu$  has the most significant effect on the runout,  $\xi$  is less sensitive and volume changes (up to +100 %) are in between. A similar pattern was observed for the Gesäuse test site.

In summary we found that a change in event magnitude up to + 100 % of the observed last relevant debris flow event has only limited consequences for hazard zones at the Pitztal and Gesäuse site and falls in the range of uncertainty of model parameterization. For the Wartschenbach site (modelled with Flo2D) variations of event magnitude showed consequences only when existing mitigation measures were neglected. We generally found that model sensitivity decreases in the order Flo2D – DAN3D – RAMMS-DF.

In order to assess the reliability of debris flows mitigation infrastructures at Wartschenbach torrent under different CC scenarios, we have performed a stochastic life cycle assessment (LCA) to estimate the expected losses. For this the results from all WPs (e.g. changes of DF frequency, scenario-based process modelling, socio-economic analysis) and archival sources (e.g. damage costs, costs for mitigation measures,...) were connected (Ballesteros et al., in prep.). The LCA takes into account: 1) the failures in the mitigation infrastructures (i.e. damages in the town) under three climatic scenarios (current, best CC scenario, worst CC scenario), and 2) related costs to maintain the infrastructures in appropriate state. This approach has allowed comparing two scenarios: the current alternative and the alternative previously to the intense event in 1997, where only limited mitigation measures were present. Results indicate that the occurrence of debris flows may change under CC scenarios, which clearly will have an important impact on the maintenance works at Wartschenbach infrastructures. The comparison between A1 (present conditions) and A2 (previous to 1997) allows concluding that the current alternative is more reliable and is based on efficiency criteria. A continued monitoring and inspection, as well as the appropriate clearance work of the system are needed to minimize the risk of check dam break this event.

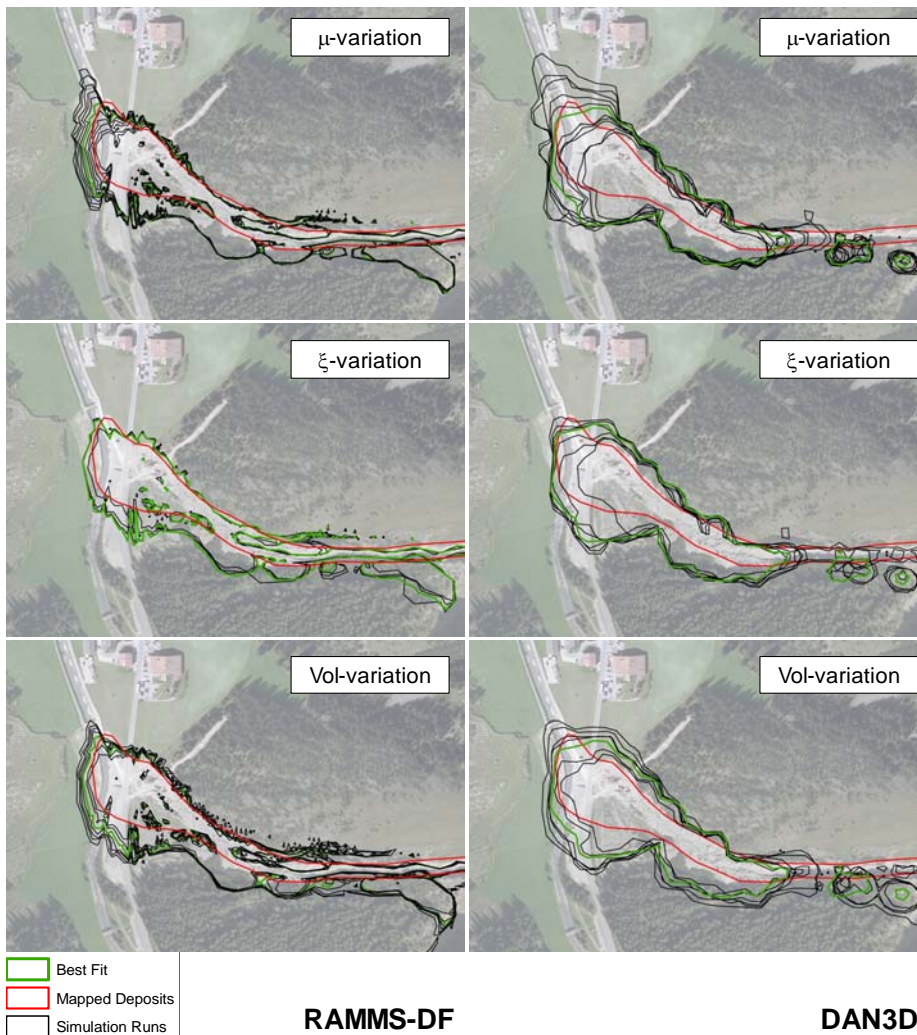


Figure 9: Variation of the Voellmy parameters ( $\mu$  and  $\xi$ ) and the initial volume for the RAMMS-DF and the DAN3D code at the Pitztal study area. Outlines of the simulation runs are given in black, respectively the best fit simulation in green. The mapped deposits of the event in 2009 are presented in red.

## 5 Schlussfolgerungen und Empfehlungen

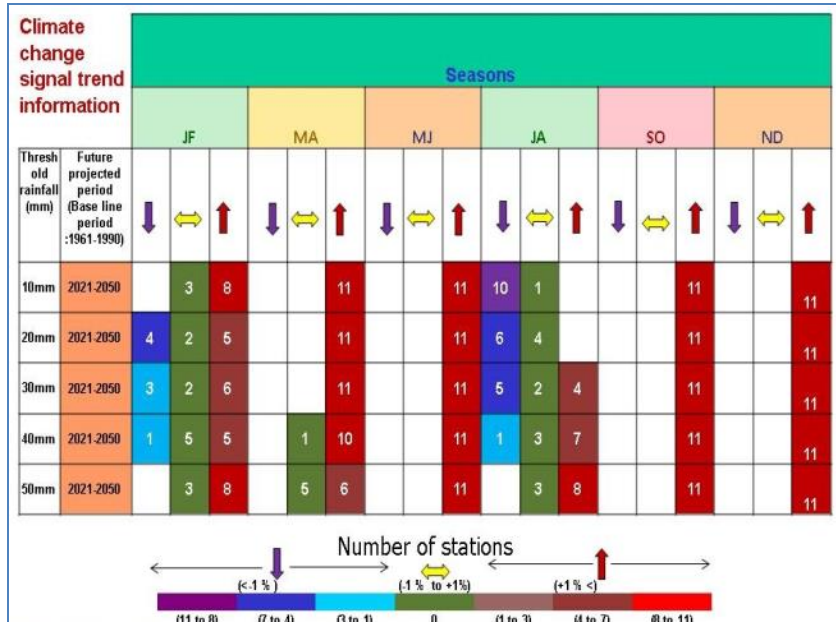
### Extreme precipitation:

There is a trend of a seasonal shift of extreme precipitation towards the shoulder seasons, i.e. May-June and September-October. We found that even for climate scenarios of decreasing total precipitation sum and decreasing frequency of "mild extremes", the frequency of very heavy precipitation extremes can increase.

The climate change signal for all stations under consideration is summarized in Table 3.

Increasing, decreasing and no change (+1% to -1%) is indicated in order to give an overview of the results for different thresholds and seasons. Different colors represent the numbers of stations. Climate change signal of single day events shows that potential triggering precipitation events are expected to become more frequent in most seasons and stations except July and August. This indication for more extreme precipitation events is most abundant in May, June, Sept., Oct., Nov., and Dec. However, also in the summer months July and August the frequency of very intense precipitation events (above 30 mm/day) often even increases. This illustrates that even under conditions with decreasing total precipitation sum and decreasing frequency of "mild extremes", the frequency of very heavy precipitation extremes can increase.

Table 3: Summary of climate change signal information of the scenario period 2021-2050 compared to 1961-1990. The number of stations with increasing (arrow up), decreasing (arrow down), and no change (horizontal arrow) in extreme precipitation frequency for different thresholds is shown



### Meteorological threshold conditions

In the Deucalion project we present for the first time a systematic analysis of triggering rainfall events for several regions in Austria, based on a large number of debris flow events and meteorological stations. By this we derived ID relations for wide regions in Austria (Table 1). We see that minimum absolute 1-day precipitation thresholds vary between 19 and 35 mm, while minimum 5-day precipitation threshold range between 3.3 and 16 mm though reproducing the negative exponent. Generally, higher thresholds are computed in the central and southern parts of Tyrol (Kitzbuhel, Lienz). Our results are comparable to those obtained with less data from Carinthia and Eastern Tyrol (Moser and Hohensinn, 1983) and in several alpine regions (e.g. NE Alps in Italy - Paronuzzi et al.,1998; Figure 10).

### Changes of torrential activity

Debris flow frequency: in the past the number of events in May-June ranged between 2 (region Liezen) and 7 events/decade (region Pitztal). In the future, according to the best scenario, no significant change will be observed. Conversely, referring to the worst scenario, the number of expected events will range between 2.1 events/decade (region Liezen) and 7 events/decade for the region representative for Kirchenlandl.

Uncertainties still exist about the evolution of debris flows in June-July. Indeed, in the past, the number of events in the past ranged between 7.6 (Liezen) and 12.8 events/decade (Gstatterboden). In the future, according to the best RCM scenario, the number of events will decrease (5.4 events/decade in Liezen and 8.1 events/decade in Gstatterboden/Gesäuse region). Conversely according to the worst scenario, changes will be observed, especially in Gesäuse area (15.9 events/decade in Admont, +76%; 21.2 events/decade in Gstatterboden, +68%; 17.1 events/decade in Kirchenlandl, +62%).

For the subsequent scenario-based hazard and risk modelling of we define scenarios of future event volumes due to CC with + 25 %, and additionally a worst case scenario of + 100 %.

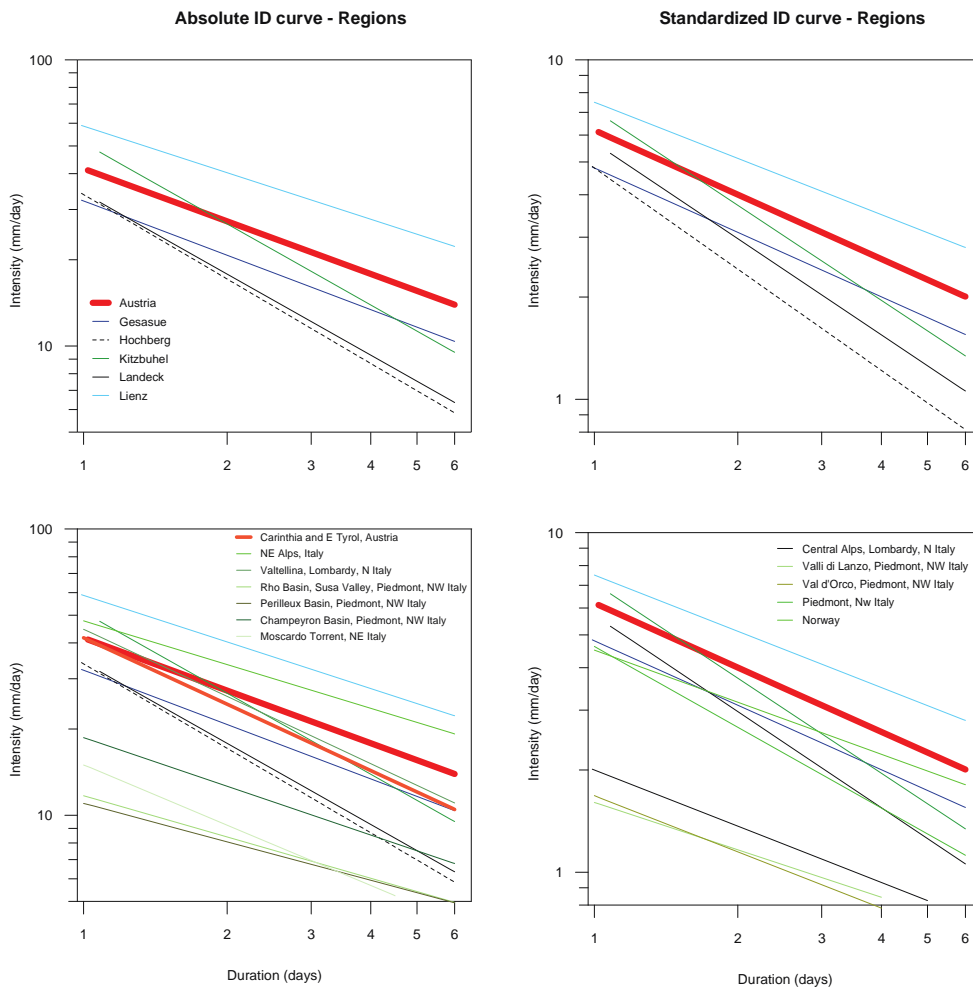


Figure 10: The obtained absolute and normalized threshold (upper panel) in comparison to a selection of other regional and local alpine ID thresholds (lower panel).

### Engineering implications

In summary we found that a change in event magnitude up to + 100 % of the observed last relevant debris flow event has only limited consequences for hazard zones at the Pitztal and Gesäuse site and falls in the range of uncertainty of model parameterization. For the Wartschenbach site variations of event magnitude showed consequences only when existing mitigation measures were neglected. We generally found that engineering simulation model sensitivity decreases in the order Flo2D – DAN3D – RAMMS-DF.

By developing a procedure of a combined Life-Cycle and risk assessment we quantify the changes of costs due to climate change scenarios on the basis of the Wartschenbach test site. We see a significant variation of risk due to different CC scenarios. Our results highlight the effect of structural mitigation measures and the importance of maintenance works.

## B) Projektdetails

### 6 Methodik

#### Dendrogeomorphology

For the reconstruction of past events, the method of dendrogeomorphology was applied. Based on a created geomorphic map and an inspection of their morphology, trees obviously influenced by past torrential activity were identified and sampled with an increment borer. At least two samples were taken per tree (see Stoffel and Bollschweiler 2008 for details on the sampling strategy). In addition, a limited number of trees were felled and cross-sections taken. The position of each sampled trees was determined on the geomorphic map. In total, 754 samples (370 increment cores, 14 cross-sections) were selected from 384 trees at the five cones.

Samples were then prepared and analyzed following the standard dendrogeomorphic procedures as described in Stoffel and Bollschweiler (2008, 2009). Individual working steps included drying and sanding of the samples, counting of tree rings and measuring ring widths. Subsequently, growth curves were cross-dated with local reference chronologies to correct faulty tree-ring series from disturbed samples and to separate natural variability (e.g., climate, insect breaks or damage caused by forest work) from growth disturbances (GD) induced by torrential processes. Within this study, we focused on the presence of (i) scars, callus tissue and tangential rows of traumatic resin ducts (TRD) as a sign of mechanical impacts, (ii) compression wood reflecting unilateral pressure and tilting of stems, (iii) sudden growth suppression following decapitation, loss of branch material, exposure of roots or deposition of material at the stem base, and (iv) the presence of growth releases in tree-ring records caused by stem burial.

The dating of past events was based on the number of trees showing a growth disturbance within the same year, the intensity of the tree-ring signal and the position of the disturbed trees, following the approach initially proposed by Shroder et al. (1978) and adapted by Kogelnig-Mayer et al. (2011) and Schneuwly-Bollschweiler et al. (2013).

#### Threshold conditions:

As described earlier, debris flow data have been extracted from a database and stored within a GIS point layer providing information location and time of occurrence. Within the database, 3947 debris flow events are recorded. Amongst these dataset, 1907 events were used for this study all of which had time accuracy of 1 day or less.

The hydro-meteorological conditions in advance of each debris flow were extracted from a dense meteorological network composed of 48 meteorological stations covering the period 1895-2011 with a daily resolution. Each catchment was associated to the closest meteorological station of this network. As, on days with temperatures below 5°C, the amount of water provided by precipitation is temporarily stored as snow in the upper part of the catchments, the events that occurred during snowy days were removed from the analysis. For information regarding the precipitation day normal (PDN) we used for normalization:  $PDN = MAP/APD$ , where MAP is the mean annual precipitation and APD the average number of precipitation days per year.

To define a valid intensity-duration (ID) threshold, it is necessary to determine the critical intensities related to durations of the rainfall events, which triggered debris flows. The choice of the duration is often done by a subjective definition of the triggering events, e.g., from the approximate point in time where heavy rainfall started (Guzzetti et al., 2007). In order to define event durations more objectively, we extracted as suggested by Meyer et al. (2012) the relevant time-dependent data directly from the meteorological dataset. Thereby we obtained the critical duration by using the maximum average intensity [ $\text{mm day}^{-1}$ ] prior to each debris flow event, also known as the maximum antecedent water supply. We used  $ID = \max(WSC / D) \sim D$ , where ID is the intensity-duration relationship used for threshold definition, WSC is the cumulative water supply in the time period prior to the debris flow and D is the corresponding duration in

days. Intensity-duration relationships were calculated for each day in 6 days in advance of each debris flow event and the maximum value was chosen for threshold definition. The intensity-duration (ID) relationships for the 1907 debris flow events served as input for the definition of minimum, medium and maximum thresholds.

All three threshold levels are calculated for the absolute and normalized intensities over a range of 1 to 6 days and can only be applied over this period of time. Power laws of the form  $I = a * D^b$  are the most common forms for ID threshold curves described in the literature (Guzzetti et al., 2007; Brunetti et al., 2010). The ID relationships defined by this function are linear in a log-log plot. The absolute threshold plot shows the absolute intensity [mm day<sup>-1</sup>] over the corresponding duration, while the normalized plot shows the absolute intensity [mm day<sup>-1</sup>] divided by the local precipitation day normal (PDN) and plotted against the duration. As noted before, normalization was carried out to account for differences in local climate.

The minimum threshold was obtained by calculating the 5th and the 15th intensity percentiles for 1 to 6 days duration. The method used for the definition of the medium and maximum thresholds was similar. The medium threshold aims to capture 50 % of the obtained ID relationships. The maximum threshold aims to capture 10 % of the ID relationships. Comparable approaches that use percentile regressions for threshold definition are performed by, e.g., Guzzetti et al. (2007) and Saito et al. (2010).

Within DEUCALION, the minimum threshold is interpreted as the "safety threshold", the lowest intensity-duration relation that is able to trigger debris flows. The medium threshold is interpreted as the intensity-duration relation that is likely to trigger debris flows, whereas the maximum threshold indicates the intensity above which debris flows will always occur. The three threshold levels are marked by the color code green, orange and red.

### Climate Modeling

#### *RCM and observational data:*

Daily mean RCM data were derived from the multi-model data-set of the ENSEMBLES project (van der Linden and Mitchell, 2009). The RCMs have a horizontal grid-spacing of 25 km and cover entire Europe. Four simulations are analyzed in detail: The RCA3 RCM driven by the HadCM3Q16 global climate model (GCM) performed at C4I (Community Climate Consortium for Ireland), the REGCM3 RCM which was driven by the ECHAM5-r3 GCM performed at the ICTP (Italian Centre for Theoretical Physics), the HIRHAM RCM which was driven by the HadCM3Q0 GCM, performed at the METNO (Norwegian Meteorological Institute), and the RCA RCM driven with the BCM GCM, performed at the SMHI (Sweden's Meteorological and Hydrological Institute). Compared to other ENSEMBLES simulations C4I-RCA3 shows a strong warming and wetter conditions in our study region, ICTP-REGCM3 shows little warming and drier conditions, METNO-HIRHAM shows moderate warming and moderate change in precipitation, and SMHI-RCA shows little warming and wetter conditions in the future (Wilcke et al., 2012). 11 stations were used in DEUCALION project and are used as an observational reference here. The station data is available in daily time steps and for the period 1971-2007.

#### *Quantile mapping:*

In the present study, a new QM version (QM<sub>β</sub>) was developed by combining parametric and nonparametric bias correction methods. The new method replaces the empirical cumulative density functions (ECDFs) by a combination of an ECDF and a generalized Pareto distribution (GPD) to preserve the major part of the empirical distribution, but to also sensibly extrapolate to new extremes.

The classical non parametric QM method is constructed as follows:

$$Y = F_{obs}^{-1}(F_{mod}(X))$$

Where F is a ECDF and F<sup>-1</sup> is the inverse function, which is named quantile function. The subscripts obs and mod indicate distributions that correspond to observed and modeled data respectively. The probability of observing X millimeter per day (or less) in the model is thus transferred to the quantile of the observed ECDF, matching exactly this probability. Y is the corrected precipitation value. In this non-parametric method, the correction of new extremes was realized by applying the correction value of the highest observed quantile, as suggested by Boé et al., (2007) and evaluated by Themeßl et al. (2012). This method will be referred hereafter as QM<sub>α</sub>.

The new method combines parametric and non-parametric bias correction approaches. Parts of the ECDFs are replaced by a generalized Pareto distribution (GPD). The distribution is divided into two parts separated by the 95th percentile as proposed by Yang et al., (2010). Values smaller than the 95th percentile are assumed to follow the empirical distribution, whereas values larger than this threshold are assumed to follow a GPD.

$$F(X; \alpha, \xi) = 1 - \left[1 + \frac{\xi X}{\alpha}\right]^{-1/\xi}$$

$$Y = \begin{cases} F_{\text{obs,emp}}^{-1} \left( F_{\text{mod,emp}}(X) \right), & \text{if } X < 95^{\text{th}} \text{ Percentile} \\ F_{\text{obs,GPD}}^{-1} \left( F_{\text{mod,GPD}}(X) \right), & \text{if } X \geq 95^{\text{th}} \text{ Percentile} \end{cases}$$

There are three parameters for estimation of GPD: a scale parameter ( $\alpha$ ), a shape parameter ( $\xi$ ), and a threshold ( $\mu$ ). The GPD is defined on  $\{X: X > 0 \text{ and } (1 + \xi X / \alpha > 0)\}$  with threshold  $\mu$  and excess  $X = z - \mu$ , where  $z$  is the observational or model data. We adopted the maximum likelihood (ML) method for estimating the parameters (e.g., Cloes 2001). Palutikof et al., (1999) found that the ML method provides stable parameter estimates over a range of thresholds. The GPD is fitted to values exceeding a selected threshold for both model as well as observational data. It has to be noted that the 95th percentile threshold value is different for the observations and the model.

Therefore, it may happen that  $X > 95^{\text{th}}$  percentile of the observations, but at the same time  $X < 95^{\text{th}}$  percentile of the model. In such a situation,  $X$  is not regarded as an extreme value.

The shape parameter  $\xi$  is responsible for "weight" of the tail of the distribution. There are three distinctive regions of the GPD distribution depending on the sign of  $\xi$  if  $\xi > 0$ , the GPD is concave and has no finite bound; if  $\xi = 0$ , the GPD is a straight line with no finite bound; if  $\xi < 0$ , the GPD is convex with an asymptotic (bounded) limit. Since a GPD with negative shape parameter has an upper bound (Coles, 2001), it limits the extrapolation of new extremes. It was observed that negative values of  $\xi$  can result in unrealistic high correction values. Two mitigate this problem and to ensure to capture the whole range of new extremes of future scenarios, we set lower bound of shape parameter to zero, similar to Kallache et al. (2011). This constraint is in general suitable for stream flow or precipitation data (Reiss and Thomas, 1997; Katz, 2002; Katz et al., 2002). The new method without controlling shape parameter and with controlling shape parameter is referred hereafter as QM $\beta$ 0, QM $\beta$ 1, respectively.

### Changes of thresholds

For the future, projections from 24 different scenarios (22 Regional Climate Models (RCM) from ENSEMBLES and 2 RCM from RECLIP) were available for 10 meteorological stations, for 2 months periods to fully assess the range of climate model uncertainty. Results present changes (in percent) in the number of days with >10 to 100 mm daily liquid precipitation.

In order to make predictions about the number of events in a future climate, events in 30, 50 and 100 km buffers around each meteorological station have been extracted from the historical database. The 100 km buffer is the only one that has been retained. Indeed, it permitted to associate a sufficient number of torrents to each meteorological station and to derive statistically significant relationships between precipitation threshold exceedance and debris flow triggering in past and future climates. In order to homogenize the dataset, only events during the period 1950-2000 were retained from the historical database. In each 100km buffer, the average rainfall intensity [mm day<sup>-1</sup>] from 1 to 3 days prior to each debris flow event was computed.

For each threshold (from 10 to 100 mm) and for each duration (from 1 to 3 days), the number of events over threshold was computed. Finally, the number of events in a future climate was predicted according to the best and worst scenarios by multiplying the number of events over thresholds by the number of events predicted by these scenarios.

### Debris flow modeling

In this study the simulation programs RAMMS-DF (Rapid Mass Movements – Debris Flow), DAN3D (Dynamic Analysis of Landslides in Three Dimensions) and Flo2d were applied. All programs provide predictions of the flow and deposition behavior of gravitational driven mass movements

like debris flows. For the 2d modeling in a 3d alpine terrain, both simulation tools require a grid based digital elevation model (DEM), information on the release area & height, as well as some individual images (e.g. areal pictures, maps) for a visualization of the results. The classic Flo2d model is well known (O'Brien et al. 1993), thus here we concentrate on the new tools RAMMS-DF and DAN3d. The simulations are based on depth-averaged shallow water equations using the Voellmy-type resistance law. (Voellmy, 1955; Salm, 1966). The DAN3D code allows a modeling selection of different types of resistance laws, like a laminar, turbulent, plastic, Bingham, frictional or Voellmy rheology. (Hungar and McDougall, 2009 and references in there). Within this study only the Voellmy rheology was applied. Here total resistance is divided into two parts: a Coulomb-type friction (coefficient  $\mu$  [-]) that scales with the normal stress and a velocity squared drag coefficient  $\xi$  [ $\text{m/s}^2$ ]. The total resistance  $S$  (Pa) is then:

$$S = \mu \rho H g \cos \varphi + (\rho g U^2) / \xi$$

where  $\rho$  is the bulk density,  $g$  is gravitational acceleration,  $\varphi$  is the slope angle,  $H$  is the flow height and  $U$  is the flow velocity.

As initial condition we used a mass block release for both simulation models. Without further information, we assumed source volumes in the upper part of catchments according to the observed deposition volumes. Sediment entrainment along the channel was neglected. The grid resolution of the simulations were set to 2 m for both, DAN3D and RAMMS-DF. By calibrating both models, best-fit simulations were carried out in a first step and provide the basis for our further investigations regarding the sensitivity of the model input parameters.

For further investigations we delineated the forested area beside the channel. We assumed increased  $\mu$  values for the forested areas to include the resilience of trees against the impact of debris flows.

Sensitivity analyses were performed for all study areas. For this we used two different criteria: runout length and deposition area. Through superposition of our simulation results over the mapped area we defined subareas that consequently give indication on the quality of the model outcome. The subareas  $A_x$ ,  $A_y$  and  $A_z$  were then related to the observed deposition area resulting in the following ratios:  $\alpha = A_x / A_{\text{mapped}}$ ,  $\beta = A_y / A_{\text{mapped}}$ , and  $\gamma = A_z / A_{\text{mapped}}$  (Figure 11). Consequently a coverage index ( $\Omega V$ ) can be evaluated that gives indication on the quality of the simulation pattern with  $\Omega V = \alpha - \beta - \gamma$

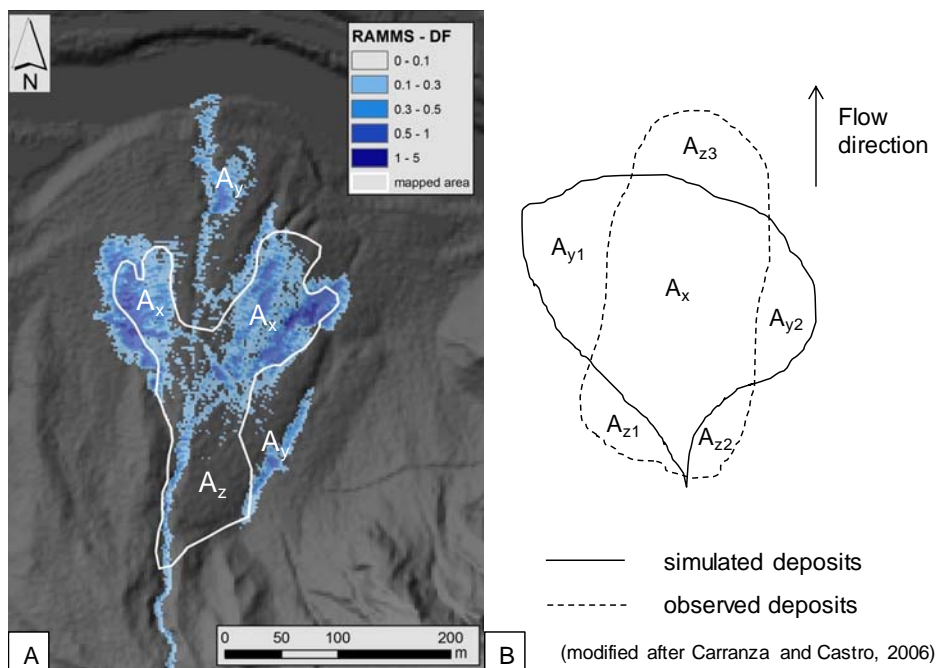


Figure 11: Superposition of the simulated area with the mapped area of recently deposited debris flow material at the Festeticgraben-cone, Gesäuse (A). Subareas where derived through overlapping the simulated deposits with the observed deposits (B).  $A_x$  represents the simulated

deposits within the mapped area whereas AZ indicates the non-simulated debris flow deposits within the observed area. Simulated deposits outside the mapped area are shown as AY.

### Life-cycle and risk assessment

A LCA analysis for each climate scenario in different alternatives has been carried out for the test site Wartschenbach using the tool 2Rsoft developed by the University of Los Andes (Sanchez Silva et al., 2011). In this approach, debris flows events are considered shocks in the system defined with a certain frequency ( $X_i$ ). The size of these shocks are related with their expected magnitude and are considered to reduce the capacity of resistance of the system ( $D(t)$ ). The LCA describe the performance (i.e., deterioration) of the system throughout its lifetime. In a life-cycle model, once a structure is put in service damage starts accumulating as a result of progressive deterioration or sudden events (i.e., shocks) until the structure fails; it is then repaired or reconstructed and the process restarts (Figure 12). The expected cost, as consequence the estimation of the related risk associated for each alternative, here is considered as the sum of all cost incurred in entire life of the infrastructure, where can be included cost for implementation, repaired works and cost related with the failure of the system.

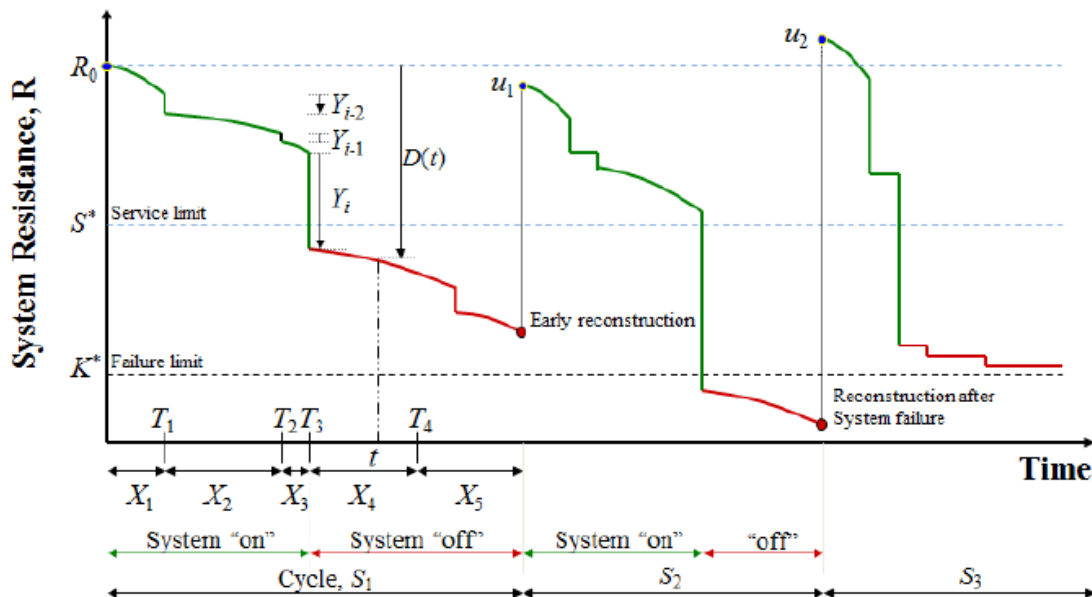


Figure 12: General description of the system remaining lifetime



## 8 Publikationen und Disseminierungsaktivitäten

### ISI-listed publications out of the Deucalion project:

- Gobiet, A., S. Kotlarski, M. Beniston, G. Heinrich, J. Rajczak, and M. Stoffel (2014), 21st century climate change in the European Alps - A review, *Sci. Total Environ.*(doi:http://dx.doi.org/10.1016/j.scitotenv.2013.07.050).
- Wilcke, R., T. Mendlik, and A. Gobiet (2013), Multi-variable error correction of regional climate models, *Clim. Change*, 120(4), 871-887 (doi:10.1007/s10584-013-0845-x).
- Schraml, K., Kogelnig, B., Scheidl, C., Stoffel, M., Kaitna, R. (2013): Estimation of debris flood magnitudes based on dendrogeomorphic data and semi-empirical relationships. *Geomorphology* 201, p.80-85 (doi: 10.1016/j.geomorph.2013.06.009).
- Kogelnig-Mayer, B., Stoffel, M., Schneuwly-Bollschweiler, M., Hübl, J., Rudolf-Miklau, F. (2011): Possibilities and Limitations of Dendrogeomorphic Time-Series Reconstructions on Sites Influenced by Debris Flows and Frequent Snow Avalanche Activity, *Arctic, Antarctic, and Alpine Research*, Vol. 43, No. 4, 2011, pp. 649–658 (DOI: 10.1657/1938-4246-43.4.649)
- Kogelnig-Mayer, B., Stoffel, M., Schneuwly-Bollschweiler, M. (2013): Four-dimensional growth response of mature *Larix decidua* to stem burial under natural conditions. *Trees* 27:1217–1223 (DOI 10.1007/s00468-013-0870-4)

### Other publications out of the Deucalion project (conference proceedings, stakeholder journals)

- Eckhart, T., Hrachowitz, M., Gobiet, A., Themessl, M., Satyanarayana, T., Schraml, K., Kaitna, R. (2013): Abschätzung möglicher Auswirkungen des Klimawandels auf das Abflussverhalten eines Wildbacheinzugsgebietes in Österreich. *Österreichische Forstzeitung*. 124. Jg., H. 6.
- Schraml, K., Oismüller, M., Kogelnig, B., Kaitna, R., Stoffel, M., Schneuwly-Bollschweiler, M (2012): Rekonstruktion von Wildbachereignissen im Gesäuse. *Österreichische Forstzeitung*, 123. Jg., H. 5, 16-17.
- Schraml, K., Thomschitz, B., McArdell, B., Graf, C., Hungr, O., Kaitna, R. (2014): Modeling debris-flow runout patterns on forested alpine fans with different dynamic simulation models. In G. Lollino et al. (eds.), *Engineering Geology for Society and Territory – Volume 2*. Springer International Publishing, Switzerland (doi: 10.1007/978-3-319-09057-3\_297).

### Presentations at external events:

- Kogelnig, B; Egginger, T; Oismüller, M; Schraml, K; Wolfsgruber, M; Schneuwly-Bollschweiler, M; Stoffel, M; Gobiet, A; Sinabell, F; Kaitna, R (2011): Assessment of Climate Change Impacts on Torrential Disasters: The Deucalion Project. 12. Österreichischer Klimatag, Universität für Bodenkultur, Wien. (Poster)
- Schraml K., Kogelnig B., Egginger T., Oismüller M., Wolfsgruber M., Corona C., Schneuwly-Bollschweiler M., Stoffel M., Gobiet A., Themessl M., Tani S., Sinabell F., Kaitna R. (2012): Assessment of Climate Change Impacts on Torrential Disasters: The Deucalion Project. 13. Österreichischer Klimatag, Universität für Bodenkultur, Wien (Poster).
- Kogelnig, B; Egginger, T; Oismüller, M; Schraml, K; Wolfsgruber, M; Schneuwly-Bollschweiler, M; Stoffel, M; Gobiet, A; Sinabell, F; Kaitna, R (2012): Assessment of climate change impacts on torrent disasters - the ACRP deucalion project. [12th Congress INTERPRAEVENT 2012, Grenoble, 23.-26. April 2012] In: Kobltschnig, G.; Hübl, J.; Braun, J. (Eds.), *Extended Abstracts*, S. 218-219, ISBN 978-3-901164-18-7 (Poster)

- Themeßl M., Mendlik T., Gobiet A, (2012): Error correction of precipitation extremes: performance and implications for scenarios, AMS Abstract # 197152, 92nd Annual meeting of the American Meteorological Society (AMS), 26th Conference on Hydrology, New Orleans, USA.
- Kaitna, R., Schraml, K., Eckhart, T., Kogelnig, B., M., Corona C., Schneuwly-Bollschweiler M., Stoffel M., Gobiet A., Themeßl M., Satyanarayana, T., Sinabell F., (2013): Abschätzung der Auswirkungen des Klimawandels auf Wildbachgefahren - Projekt Deucalion. 14. Österreichischer Klimatag, Universität für Bodenkultur, Wien. (Poster)
- Schraml K., McArdell B.W., Graf C., Stoffel M., Kaitna R. (2013): Assessment of the frictional effect of forests on debris flow runout in numerical models. Geophysical Research Abstracts Vol. 15, EGU2013-9873. EGU General Assembly 2013. (Poster)
- Eckhart, T., Hrachowitz, M., Gobiet, A., Themessl, M., Satyanarayana, T., Kaitna, R. (2013): Estimation of climate change impact on the runoff from a small alpine watershed in Austria. Geophysical Research Abstracts Vol. 15, EGU2013-11681. EGU General Assembly 2013 (Poster)
- Satyanarayana, T., Themessl, M., Gobiet, A. (2013): Empirical-statistical downscaling and error correction of extreme precipitation from regional climate models. Geophysical Research Abstracts Vol. 15, EGU2013-5889. EGU General Assembly 2013 (Poster)
- Kaitna, R., Schraml, K., Stoffel, M., Corona, C., Ballesteros, J., Gobiet, A., Satyanarayana, T., Sinabell, F. (2014): Assessment of Climate Change Impacts on Torrential Disasters: The Deucalion Project. 15. Österreichischer Klimatag, Universität für Bodenkultur, Wien.(Presentation)
- Schraml, K., McArdell, B.W., Graf, C., Thomschitz, B., Kaitna, R. (2014): Evaluating Voellmy resistance parameters for debris-flow simulation models. Geophysical Research Abstracts, EGU2014-7332. EGU General Assembly 2014. (Presentation).
- Braun, M., Huebl, J., Kaitna, R. (2014): Connecting a large database of debris flow events in Austria with daily precipitation data. Geophysical Research Abstracts EGU2014-3796. EGU General Assembly 2014 (Poster).
- Schraml, K., Thomschitz, B., McArdell, B., Graf, C., Hungr, O., Kaitna, R. (2014): Modeling debris-flow runout patterns on forested alpine fans with different dynamic simulation models. IAEG XII Congress 2014 (presentation)

Diese Projektbeschreibung wurde von der Fördernehmerin/dem Fördernehmer erstellt. Für die Richtigkeit, Vollständigkeit und Aktualität der Inhalte übernimmt der Klima- und Energiefonds keine Haftung.

## References:

- Boé J, Terray L, Habets F, Martin E. (2007): Statistical and dynamical downscaling of the Seine basin climate for hydro-meteorological studies. *International Journal of Climatology* 27: 1643–1655.
- Brunetti, M. T., Peruccacci, S., Rossi, M., Luciani, S., Valigi, D., and Guzzetti, F. (2010): Rainfall thresholds for the possible occurrence of landslides in Italy, *Nat. Hazards Earth Syst. Sci.*, 10, 447–458, doi:10.5194/nhess-10-447-2010.
- Carranza, E. J. M. und Castro, O. T. (2006): Predicting lahar-inundation zones: Case study in West Mount Pinatubo, Philippines. *Natural Hazards*, 37, 331–372
- Christen, M., Kowalski, J., Bartelt, P. (2010): RAMMS: Numerical simulation of dense snow avalanches in three-dimensional terrain. *Cold Regions Science and Technology*, Vol. 63, 1-2, pp. 1 – 14.
- Coles S (2001). An introduction to statistical modeling of extreme values. Springer, Berlin, p 224
- Dobler A, Ahrens B. (2008): Precipitation by a regional climate model and bias correction in Europe and South Asia. *Meteorologische Zeitschrift* 17: 499–509.
- Eckhart, T., Hrachowitz, M., Gobiet, A., Themessl, M., Satyanarayana, T., Schraml, K., Kaitna, R. (2013): Abschätzung möglicher Auswirkungen des Klimawandels auf das Abflussverhalten eines Wildbacheinzugsgebietes in Österreich. *Österreichische Forstzeitung*. 124. Jg., H. 6.
- Fuchs, S. und A. Zischg (2013): Vulnerabilitätslandkarte Österreich, IAN Report 152, Institut für Alpine Naturgefahren, Universität für Bodenkultur (unveröffentlicht).
- Guzzetti, F., Peruccacci, S., Rossi, M., and Stark, C. P. (2007): Rainfall thresholds for the initiation of landslides in central and southern Europe, *Meteorol. Atmos. Phys.*, 98, 239–267.
- Hungr, O., McDougall, S. (2009): Two numerical models for landslide dynamic analysis. *Computers & Geosciences* 35 (5), 978–992.
- IPCC. 2001. *Climate Change 2001. The Scientific Basis. Contribution of Working Group I to the Third Assessment Report of the Intergovernmental Panel on Climate Change* [Houghton JT, Ding Y, Griggs DJ, Noguer M, van der Linden PJ, Dai X, Maskell K, Johnson CA (eds.)]. Cambridge University Press. Cambridge, New York.
- IPCC. 2007. *Climate Change. Contribution of Working Group I to the Fourth Assessment Report of the Intergovernmental Panel on Climate Change, 2007* [Solomon, S., D. Qin, M. Manning, Z. Chen, M. Marquis, K.B. Averyt, M. Tignor and H.L. Miller (eds.)] Cambridge University Press. Cambridge, New York.
- Kallache, M., M. Vrac, P. Naveau, and P.A. Michelangeli (2011), Nonstationary probabilistic downscaling of extreme precipitation, *J. Geophys. Res.*, 116, D05113, doi:10.1029 /2010JD014892.
- Katz, R. W. (2002), Techniques for estimating uncertainty in climate change scenarios and impact studies, *Clim. Res.*, 20, 167–185.
- Katz, R. W., M. B. Parlange, and P. Naveau (2002), Statistics of extremes in hydrology, *Adv. Water Resour.*, 25, 1287–1304.
- Kogelnig-Mayer, B., Stoffel, M., Schneuwly-Bollschweiler, M., Hübl, J., Rudolf-Miklau, F. (2011): Possibilities and Limitations of Dendrogeomorphic Time-Series Reconstructions on Sites Influenced by Debris Flows and Frequent Snow Avalanche Activity, *Arctic, Antarctic, and Alpine Research*, Vol. 43, No. 4, 2011, pp. 649–658 (DOI: 10.1657/1938-4246-43.4.649).
- Meyer, N. K., Dyrddal, A. V., Frauenfelder, R., Etzelmüller, B., and Nadim, F. (2012): Hydrometeorological threshold conditions for debris flow initiation in Norway, *Nat. Hazards Earth Syst. Sci.*, 12, 3059-3073, doi:10.5194/nhess-12-3059-2012
- Moser M, Hohensinn, F. (1983): Geotechnical aspects of soil slips in Alpine regions. *Eng Geol* 19: 185–211
- O'Brien, J.S.; Julien, P.Y.; Fullerton, W.T. (1993): Two-dimensional water flood and mudflow simulation. *J. Hydraulic Engineering* 119(2): 244-261
- Palutikof JP, Brabson BB, Lister DH and Adcock ST (1999): A Review of Methods to Calculate Extreme Wind Speeds, *Meteorological Applications*, 6, 119-132.
- Piani C, Haerter JO, Coppola E. (2009): Statistical bias correction for daily precipitation in regional climate models over Europe. *Theoretical and Applied Climatology* 99 (1-2): 187–192. doi: 10.1007/s00704-009-0134-9.

- Paronuzzi P, Coccolo A, Garlatti G. (1998): Eventi meteorici critici e debris flows nei bacini montani del Friuli. *L'Acqua, Sezione I/Memorie*: 39–50
- Reiss, R. D., and M. Thomas (1997), *Statistical Analysis of Extreme Values with Applications to Insurance, Finance, Hydrology and Other Fields*, Birkhauser, Basel, Switzerland.
- Saito, H., Nakayama, D., and Matsuyama, H. (2010): Relationship between the initiation of a shallow landslide and rainfall intensity-duration thresholds in Japan, *Geomorphology*, 118, 167–175, 2010.
- Salm, B. (1966): Contribution to avalanche dynamics. *International Association of Scientific Hydrology Publication 69 (Symposium at Davos 1965 - Scientific Aspects of Snow and Ice Avalanches)*, 199–214.
- Sanchez-Silva, M., Klutke, G.-A., Rosowsky, D.V. (2011): Life-cycle performance of structures subject to multiple deterioration mechanisms. *Struct. Saf.* 33(3): 206–217
- Schneuwly-Bollschweiler, M., Corona, C., Stoffel, M., (2013): How to improve dating quality and reduce noise in tree-ring based debris-flow reconstructions. *Quaternary Geochronology* 18, 110-118
- Schraml, K., Oismüller, M., Kogelnig, B., Kaitna, R., Stoffel, M., Schneuwly-Bollschweiler, M (2012): Rekonstruktion von Wildbachereignissen im Gesäuse. *Österreichische Forstzeitung*, 123. Jg., H. 5, 16-17
- Schraml, K., Oismüller, M., Stoffel, M., Hübl, J., Kaitna, R.: Debris-flow activity in five adjacent gullies in a limestone mountain range (in review)
- Shroder, J.F. (1978): Dendrogeomorphological analysis of mass movement on Table Cliffs Plateau, Utah. *Quaternary. Research* 9, 168–185
- Sinabell, F. (2014): DEUCALION – Socio-economic Developments at Study Sites and Related Changes in Vulnerability. *Studie des Österreichischen Instituts für Wirtschaftsforschung im Auftrag des Klima- und Energiefonds*. Wien 2014.
- Sinabell, O. Fritz, W. Puwein und G. Streicher (2009): Eine volkswirtschaftliche Analyse der Wildbach- und Lawinenverbauung (an economic analysis of avalanche and torrent control measures). *Studie des Österreichischen Instituts für Wirtschaftsforschung im Auftrag des Bundesministeriums für Land- und Forstwirtschaft, Umwelt und Wasserwirtschaft*, Wien.
- Stoffel, M., Bollschweiler, M. (2008): Tree-ring analysis in natural hazards research — an overview. *Natural Hazards and Earth System Sciences* 8, 187-202.
- Stoffel, M., Bollschweiler, M. (2009): What tree rings can tell about earth-surface processes: teaching the principle of dendrogeomorphology. *Geography Compass* 3, 113-137.
- Thiemeßl, M. J., Gobiet, A., Leuprecht, A., (2011) Empirical-statistical downscaling and error correction of daily precipitation from regional climate models. *International Journal of Climatology* 31(10):1530–1544, URL <http://doi.wiley.com/10.1002/joc.2168>
- Thiemeßl, M. J., Gobiet, A., and Heinrich, G., (2012), Empirical-Statistical Downscaling and Error Correction of Regional Climate Models and its Impact on the Climate Change Signal, *Climatic Change* 112(2):449–468
- van der Linden P, Mitchell JFB. 2009. ENSEMBLES: Climate Change and its Impacts: Summary of research and results from the ENSEMBLES project. Met Office Hadley Centre. Exeter.
- Voellmy, A. (1955): Über die Zerstörungskraft von Lawinen. *Schweizerische Bauzeitung* 73, 212–285.
- Wilcke RAI, Leuprecht A, Andreas G (2012) Effects of climate change on future snow conditions in tyrol and styria (cc-snow), final report – climate. [http://www.uni-graz.at/igam7www-wcvscirep-no48-wilcke-et-al-2012\\_compressed.pdf](http://www.uni-graz.at/igam7www-wcvscirep-no48-wilcke-et-al-2012_compressed.pdf). Wegener Center Verlag, Graz, Austria
- Wilcke, R., T. Mendlik, and A. Gobiet (2013), Multi variable error correction of regional climate models, *Clim. Change*, 120(4), 871–887 (doi:10.1007/s10584-013-0845-x)
- Wilcke, R.A.I (2014) Evaluation of Multi-Variable Quantile Mapping on Regional Climate Models, PhD thesis, Wegener Center Verlag, Sci. Rep. No. 56-2014, 165 pp, ISBN, Graz, Austria, 2014.
- Yang W, Andreasson J, Graham LP, Olsson J, Rosberg J, Wetterhall F (2010) Distribution-based scaling to improve usability of regional climate model projections for hydrological climate change impacts studies. *Hydrol Res* 41:211–229. doi:10.2166/nh.2010.004